Development of cohesive models from the study of atomic scale fracture processes

P.A. Klein [a] J.A. Zimmerman [a] E.P. Chen [a]

[a] *Sandia National Laboratories, Livermore, CA 94550*

Abstract

In this work, we make a comparison of continuum simulations using a cohesive modeling approach with the predictions of atomistic simulations. Cohesive approaches to modeling fracture differ from classical approaches by embedding the physics of the fracture process directly in the simulation procedure. Cohesive zone methods use a traction-separation relationship to provide the constitutive relations for the localized failure mode of deformation. For modeling brittle fracture, the form of these traction-separation relations is typically based on simple physical arguments and motivation from semi-empirical atomistic potentials. First, we derive the parameters for the cohesive relations based on evaluation of Griffiths condition with the atomistic system. We then compare the fracture behavior predicted by this cohesive model with the results of atomistic simulations under quasistatic and dynamic loading conditions. We find that while cohesive approaches adequately reproduce the atomistic results under quasistatic loading, dynamic conditions reveal the significant effects dispersion has on the behavior of dynamically propagating cracks.

Key words: fracture simulation; atomistic simulation; cohesive modeling; multiscale modeling

1 Introduction

As early as 1933, Prandtl[3] employed a cohesive traction relation, motivated by atomistic considerations, to analyze debonding between two slender beams. Cohesive approaches to modeling fracture replace the point singularity model of the crack tip with a stress or traction response that incorporates a finite cohesive strength and a finite work to fracture. These approaches promise to reproduce the behavior of propagating cracks more accurately because the dissipation mechanisms associated growth may be directly incorporated in the cohesive relations. The approach of restricting the mechanisms of cohesive fracture to act only across discrete surfaces is gaining wide acceptance in the fracture modeling community. A finite element implementation of the cohesive surface approach was introduced by Needleman [2]. Ironically, while cohesive

approaches admit a very detailed description of crack tip processes, these processes are largely unobservable due to the small length scales involved and the relative inaccessibility of the fracture process zone. In this work, we attempt to validate the cohesive surface approach by comparison with a model atomistic system. Atomistic simulation provides physically realistic energetics and dynamics of crack growth processes that can be readily analyzed.

Depending on the material system, the fracture processes may be numerous and complicated. For this work, we consider only brittle fracture, which we define to mean that all dissipation during the fracture process is associated directly with the creation of new free surfaces. Accordingly, our continuum simulations employ a rate and history independent bulk constitutive model. The atomistic system used in this study is similar to the one considered by Farid et al. [1] to study the behavior of crack growth under severe loading conditions. Given sufficient driving force, this system activates additional mechanisms of dissipation during fracture. These include increasing the fracture surface area through roughening and relieving stresses through dislocation emission. In this study, crack driving forces are maintained below a level at which these dissipation mechanisms are activated. Therefore, we expect to understand the fracture behavior in terms of the surface dissipation and the transport of strain energy by elastic waves or dispersion by phonons for the atomistic system.

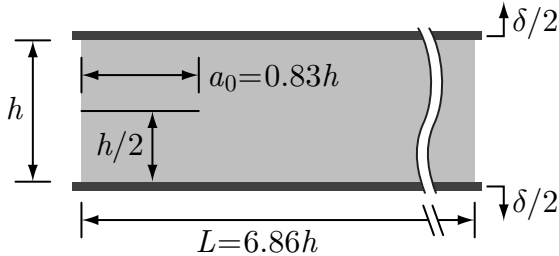The strip geometry used in this study is illustrated in Figure 1. If the strip is

Fig. 1. Geometry of the two-dimensional strip.

sufficiently long in the lateral dimension, a J-integral analysis can be used to determine the static crack driving force under plain stress as

$$G = \frac{E \, h \, \epsilon^2}{2 \, (1 - \nu^2)},$$

(1)

where E is Young's modulus, ν is Poisson's ratio, and $\epsilon = \frac{\delta}{h}$ is the nominal applied strain. This quasistatic analysis only applies to the onset of crack growth. Accurate predictions of the response of either the continuum or atomistic system during dynamic propagation remains a challenge for analysis.

2 Methods

Over a domain Ω with a boundary Γ, the variational form of the dynamic equation of equilibrium in the absence of body forces may be written as

$$\int_\Omega \rho \frac{\partial^2 \mathbf{u}}{\partial t^2} \cdot \delta \mathbf{u} \, d\Omega + \int_\Omega \boldsymbol{\sigma} : \delta \boldsymbol{\epsilon} \, d\Omega + \int_{\Gamma_{\text{int}}} \mathbf{t}(\boldsymbol{\Delta}) \cdot \delta \boldsymbol{\Delta} \, d\Gamma = \int_{\Gamma_h} \mathbf{t} \cdot \delta \mathbf{u} \, d\Gamma, \qquad (2)$$

where ρ is the mass density, $\mathbf{u}$ is the displacement field, $\boldsymbol{\epsilon} = \frac{1}{2}\left(\nabla \mathbf{u} + (\nabla \mathbf{u})^{\text{T}}\right)$ is the infinitesimal strain tensor, and the Cauchy stress $\boldsymbol{\sigma}$ and traction $\mathbf{t}$ are related through the normal $\mathbf{n}$ as $\mathbf{t} = \boldsymbol{\sigma} \mathbf{n}$. Contributions from surface tractions in (2) appear over regions of the boundary $\Gamma_h \subseteq \Gamma$ with externally applied tractions and over pairs of internal surfaces Γ_{int} due to the variation in the surface opening displacement $\delta \boldsymbol{\Delta}$. For this study, we use a model traction-separation relation similar to the one introduced by Tvergaard and Hutchinson [4]. The magnitude of the cohesive traction is expressed as a function of a nondimensional effective opening displacement

$$\Delta = \sqrt{(\Delta_t/\delta_t^*)^2 + (\Delta_n/\delta_n^*)^2}, \qquad (3)$$

where δ_t^* and δ_n^* represent the characteristic tangential and normal opening displacements, respectively. As illustrated in Figure 2(a), the tri-linear magnitude of the traction $\hat{t}(\Delta)$ depends on a single shape factor Δ^*. The traction response is assumed to be reversible up to $\Delta = \Delta^*$, after which the surface is assumed to have failed. Defining a traction potential

$$\varphi(\boldsymbol{\Delta}) = \delta_n^* \int_0^\Delta \hat{t}(\xi) \, d\xi \qquad (4)$$

yields the rate-independent, mixed-mode traction-separation relation

$$\mathbf{t}(\boldsymbol{\Delta}) = \frac{\partial \varphi(\boldsymbol{\Delta})}{\partial \boldsymbol{\Delta}} = \delta_n^* \, \hat{t}(\Delta) \, \frac{\partial \Delta}{\partial \boldsymbol{\Delta}} \qquad (5)$$

and a fracture energy

$$G_c = \frac{1}{2} \sigma_c \delta_n^*. \qquad (6)$$

The cohesive surface relation (5) is not intended to represent the response of any specific material. Surrounded by an elastic medium, the detailed shape of the relationship is not expected to have a significant effect. The relationship simply introduces a well-defined fracture energy into the simulation procedure with a clear point of complete failure in a form that facilitates analytical study. The stress response of the bulk is defined by

$$\sigma_{ij} = [\mu \, \delta_{ij}\delta_{rs} + \lambda \, (\delta_{ir}\delta_{js} + \delta_{is}\delta_{jr})] \, \epsilon_{rs}, \qquad (7)$$

where μ and λ are Lamé constants.

3

The approach for the atomistic simulations similarly makes use of a model system. The single crystal sample is constructed from a two-dimensional, hexagonal lattice bound by the Lennard-Jones 6-12 potential

$$\phi_{LJ}(r) = 4\,\varepsilon \left[-\,(\sigma/r)^6 + (\sigma/r)^{12} \right], \tag{8}$$

where σ sets the length scale of the potential and $-\varepsilon$ is the depth of the potential well. In order to allow us to control the range of influence of the potential without introducing abrupt behavior at a cut-off distance, we use the modified potential

$$\phi(r) = \phi_{LJ}(r) - \phi_{LJ}(r_c) - (r - r_c)\,\phi'_{LJ}(r_c), \tag{9}$$

where r_c is the distance at which the potential and its first derivative pass through 0. This cut-off distance is selected to include up to the fifth nearest neighbors in the undeformed configuration. The crystal is oriented with lattice vectors

$$\mathbf{r}^{(1)} = r_0 \left\{ \begin{matrix} 1 \\ 0 \end{matrix} \right\} \qquad \text{and} \qquad \mathbf{r}^{(2)} = \frac{r_0}{2} \left\{ \begin{matrix} 1 \\ \sqrt{3} \end{matrix} \right\}, \tag{10}$$

where r_0 is the interatomic spacing. We choose $\frac{h}{r_0} = 212$ to distance the fracture process zone from the rigidly imposed boundary conditions. The characteristic dimension of the finite elements near the cleavage plane is $h_{\min} = r_0$.

3   Results and discussion

The parameters for the continuum and atomistic systems are selected to correspond with each as closely as the differing descriptions permit. Due to the centrosymmetry of the undeformed lattice, the initial elastic properties of the crystal display Cauchy symmetry, for which $\lambda = \mu$. The shear modulus μ is matched to the elastic properties calculated for the crystal, and the density ρ is selected to correspond with the mass and atomic volume of the undeformed lattice. The fracture properties of the systems cannot be compared so directly. The fracture energy ϕ is not solely dependent on ε, the energy of a single bond, and the effective opening displacement Δ (3) does not correspond to the bond length r.

The fracture parameters in the cohesive relation $\mathbf{t}(\Delta)$ (5) are selected in order to match the traction distribution on the cleavage plane of the strip model at the critical boundary displacement. The critical displacement is identified by applying Griffith's condition to the atomistic system. The boundaries are displaced until the static, uncleaved configuration of the strip is no longer energetically favored. Comparing the bond energy per undeformed volume "far" ahead of the pre-crack with the reference energy of the crystals yields the fracture energy G_c. The traction distribution for the atomistic system is calculated from the force in all bonds crossing the cleavage plane, averaged over segments of length r_0 along the fracture surface. This calculation yields a peak traction

4

of approximately $E/18$, where E is Young's modulus of the crystal. Matching just these two characteristics yields traction distributions illustrated in Figure 2(b). Quasistatic analysis of the strip configuration yields a failure strain
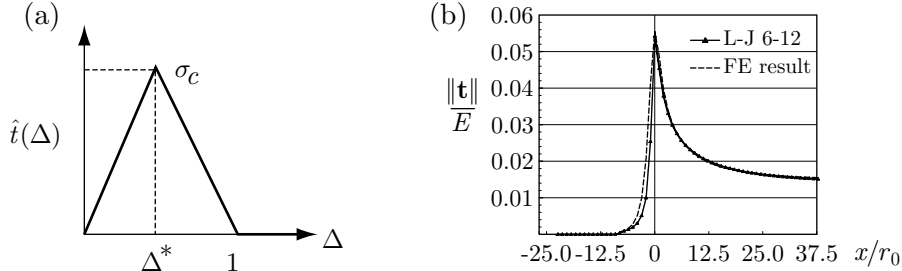

Fig. 2. (a) the traction-separation relation and (b) a comparison of the traction distribution on the cleavage plane.

$\epsilon_c = \frac{\delta}{h} \approx 1.5$ %. The continuum simulation cleaves at a strain within 1% of the predicted value. Correcting the Griffith analysis to account for the compliance of the cohesive surface layer reveals that the continuum simulation reproduces the expected failure strain to within nearly 0.1%. These results indicate that model has sufficient extent both ahead and behind the crack tip to match the steady-state cracking assumptions and that the tractions are well resolved over the elements in the fracture process zone. The atomistic model cleaved at a strain approximately 4% higher than that predicted by the Griffith analysis, which we attribute to the nonlinear response of the interatomic potentials. Figure 2(b) illustrates that the region on the traction distribution behind the peak is a tail that decays over a distance of approximately $10\,r_0$, and the stresses ahead of the tip stay well above the farfield values to a distance of nearly $25\,r_0$.

For the dynamic simulations, the continuum and atomistic system are loaded from near their critical strains with a constant velocity of $c_d/\dot{\delta} = 7500$, where c_d is the dilatational wave speed in the material. The atomistic system is loaded to near the critical strain using molecular statics, and an energy conserving conserving time integration scheme is used for the dynamic phase of the simulations. The variation of the crack velocity as a function of crack length is shown in Figure 3(a). The velocity is normalized by the Rayleigh wave speed c_R, the limit speed for cracks propagating under mode I loading. While the crack speed in the continuum simulation steadily climbs towards the limiting speed with increasing driving force, the crack speed in the atomistic simulation does not exceed approximately 20% c_R. Figure 3(b) reveals the markedly different energetics associated with crack growth for each system. The figure shows the rate of kinetic energy generation with crack extension $\frac{\Delta T}{\Delta a}$ as a function of crack length. The continuum simulation shows that approximately 3% of the strain energy required for quasistatic crack growth is converted to kinetic energy for $1 < \frac{a}{h} < 4$, corresponding to $0.2 < \frac{\dot{a}}{c_R} < 0.7$. For $\frac{a}{h} > 4$, acceleration of the crack slows and the rate of kinetic energy gener-
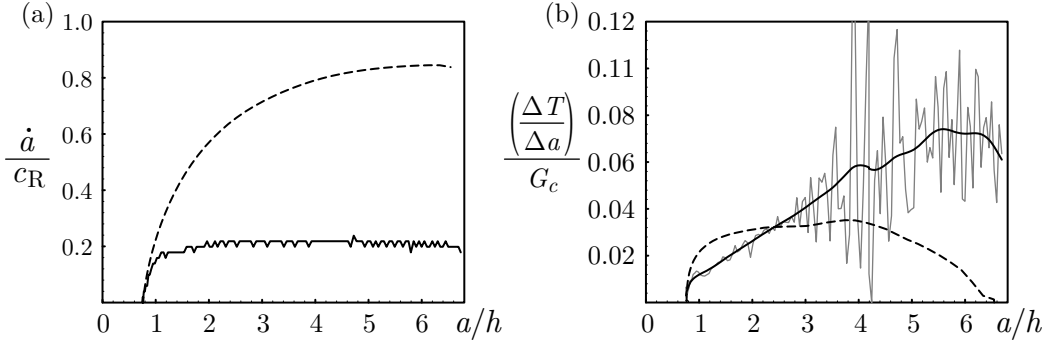
Fig. 3. Comparison of the continuum simulations with a cohesive surface interface (dashed lines) with atomistic simulations (solid lines).

ation decreases although the driving force continues to increase. The smoothed results from the atomistic simulation (dark, solid line in Figure 3(b)) reveal a steadily increasing rate of kinetic energy generation. The results suggest that the terminal crack speed for the continuum simulation is determined largely by limits in the driving strain energy release rate, while the terminal crack speed in the atomistic system is controlled by an intrinsic limit on the rate of bond breaking at the crack tip. Excess energy is converted to kinetic energy rather than increasing the speed of fracture.

In summary, we have compared the response of a continuum and atomistic system under conditions of quasistatic and dynamic fracture. Under quasistatic conditions, the cohesive surface approach reproduces the predicted response of the strip model. This result is expected since traction potential (4), with a simple change of variables, is equivalent to the J-integral evaluated on a contour over crack surfaces surrounding the tip. Under dynamic conditions, simply adopting a cohesive approach cannot reproduce crack dynamics of an atomistic system even when restricted to purely brittle propagation. We are currently assessing methods in which the continuum simulation approach can be improved to account for the dispersive behavior displayed by the atomistic system.

References

[1] F.F. Abraham, D. Brodbeck, R.A. Rafey, and W.E. Rudge. Instabilities dynamics of fracture: a computer simulation investigation. *Physics Review Letters*, 73:272–275, 1994.

[2] A. Needleman. A continuum model for void nucleation by inclusion debonding. *Journal of Applied Mechanics*, 54:525–531, 1987.

[3] L. Prandtl. Ein Gedankenmodell für den Zerreißvorgang spröder Körper. *Zeitschrift für angewandte Mathematik und Mechanik*, 13:129–133, 1933.

[4] V. Tvergaard and J.W. Hutchinson. The influence of plasticity on mixed mode interface toughness. *Journal of the Mechanics and Physics of Solids*, 41:1119–1135, 1993.